Macromolecules
ARTICLE

Macromolecules **2010**, *43*, 697–708 **697**
DOI: 10.1021/ma902206u

Synthesis and Characterization of Bridged Bithiophene-Based Conjugated Polymers for Photovoltaic Applications: Acceptor Strength and Ternary Blends

Chiu-Hsiang Chen, Chao-Hsiang Hsieh, Martin Dubosc, Yen-Ju Cheng,* and Chain-Shu Hsu*

Department of Applied Chemistry, National Chiao Tung University, 1001 Ta Hsueh Road, Hsin-Chu 30010, Taiwan

Received October 7, 2009; Revised Manuscript Received November 24, 2009

ABSTRACT: Six of three-component donor−acceptor random copolymers **P1**−**P6**, symbolized as (thiophene donor)$_m$−(thiophene acceptor)$_n$, were rationally designed and successfully synthesized by the palladium-catalyzed Stille coupling. The 4*H*-cyclopenta[2,1-*b*:3,4-*b*′]dithiophene (CPDT) unit serves as the donor for **P1**−**P4**, while the benzothiadiazole (BT), quinoxaline (QU), dithienoquinoxaline, and thienopyrazine (TP) units are used as the acceptor for **P1**, **P2**, **P3**, and **P4**, respectively. **P5** and **P6** are structurally analogous to **P1** and **P2** except for using the dithieno[3,2-*b*:2′,3′-*d*]silole (DTS) unit as the donor. Because the band gap lowering ability of the acceptor units in the polymer is in the order TP > BT > QU presumably due to the quinoid form population in the polymers, the optical band gaps can be well adjusted to be 1.2, 1.6, and 1.8 eV for **P4**, **P1**, and **P2**, respectively. It is found that the two bridged bithiophene units, CPDT and DTS, have similar steric and electronic effects on the **P1** and **P5** as well as **P2** and **P6**, respectively, leading to comparable intrinsic properties and device performances. Bulk heterojunction photovoltaic cells based on ITO/PEDOT:PSS/polymer:$PC_{71}BM$/Ca/Al configuration were fabricated and characterized. Although **P4** exhibits the lowest optical band gap, broadest absorption spectrum, and highest mobility, the too low-lying LUMO level hinders the efficient exciton dissociation, resulting in a low PCE of 0.7%. Compared with poly[2,6-(4,4-bis(2-ethylhexyl)-4*H*-cyclopenta[2,1-*b*;3,4-*b*′]dithiophene)-*alt*-4,7-(2,1,3-benzothiadiazole)] (PCPDTBT), random copolymer **P1** shows more blue-shifted, broader absorption spectrum, comparable mobility, and a higher PCE of 2.0%. In view of the fact that **P1** shows a higher band gap with strong absorption in visible region, while PCPDTBT has a lower band gap to mainly absorb NIR light, a BHJ device with the active layer containing ternary blend of PCPDTBT/**P1**/$PC_{71}BM$ was investigated and achieved an enhanced PCE of 2.5%, which outperforms the devices based on the binary blending systems of PCPDTBT/$PC_{71}BM$ (PCE = 1.4%) or **P1**/$PC_{71}BM$ (PCE = 2.0%) under the identical conditions. Such an improvement is ascribed to the complementary absorption and compatible structure of **P1** and PCPDTBT polymers.

Introduction

Harvesting energy directly from sunlight using photovoltaic technology is considered as one of the most important ways to address the growing global energy needs. Polymer solar cells (PSCs) are a promising alternative for clean and renewable energy due to its potential advantage to be fabricated onto large area, lightweight flexible substrates by solution processing at a lower cost.[1] PSCs based on the concept of bulk heterojunction (BHJ) configuration where an active layer comprises a composite of a p-type (donor) and an n-type (acceptor) materials represents the most useful strategy to maximize the internal donor−acceptor interfacial area allowing for efficient charge separation.[2] Fullerene derivatives such as [6,6]-phenyl-C_{61}-butyric acid methyl ester (PCBM)[3] have been proven to be the ideal n-type materials ubiquitously used for BHJ solar cells because of their exceptional ability to induce ultrafast electron transfer as well as excellent electron transport properties.[4] To achieve high efficiency of PSCs, one of the most critical challenges in the molecular level is to develop ideal p-type conjugated polymers that simultaneously possess (1) sufficient solubility to guarantee solution processability and miscibility with an n-type material, (2) low band gap (LBG) for strong and broad absorption spectrum extending to near-infrared to capture more solar photons, and (3) high hole mobility for efficient charge transport.

The most powerful strategy to design a LBG conjugated polymer is to incorporate electron-rich donor and electron-deficient acceptor segments in the polymer backbone. Through the push−pull interaction, efficient photoinduced intramolecular charge transfer (ICT) takes place from the donor to the acceptor upon photoexcitation, generating an absorption band at the lower energy.[5] Electron donor segments in the conjugated polymers are generally constituted by electron-rich heteroaromatic rings such as thiophene and pyrrole units. Structurally analogous to fluorene, 4*H*-cyclopenta[2,1-*b*:3,4-*b*′]dithiophene (CPDT)[6] and dithieno[3,2-*b*:2′,3′-*d*]silole (DTS),[7] where a 2,2′-bithiophene is covalently bridged and rigidified at the 3,3′-position by a carbon and a silicon atom, respectively, have attracted considerable research interest owing to their potential to serve as donor building blocks for LBG polymers.[8] Because of the fully coplanar structure, the intrinsic properties based on bithiophene can be altered, leading to more extended conjugation, lower HOMO−LUMO energy band gap, and stronger intermolecular interaction. Furthermore, the ability of functionalization at bridging carbon and silicon allows for introducing two highly solubilizing aliphatic side chains without affecting its coplanarity.

*To whom correspondence should be addressed: Ph +886-3513-1523; Fax +886-3513-1523; e-mail yjcheng@mail.nctu.edu.tw (Y.-J.C.) and cshsu@mail.nctu.edu.tw (C.-S.H.).

Published on Web 12/09/2009

Scheme 1. Chemical Structures of PCPDTBT and P1−P6

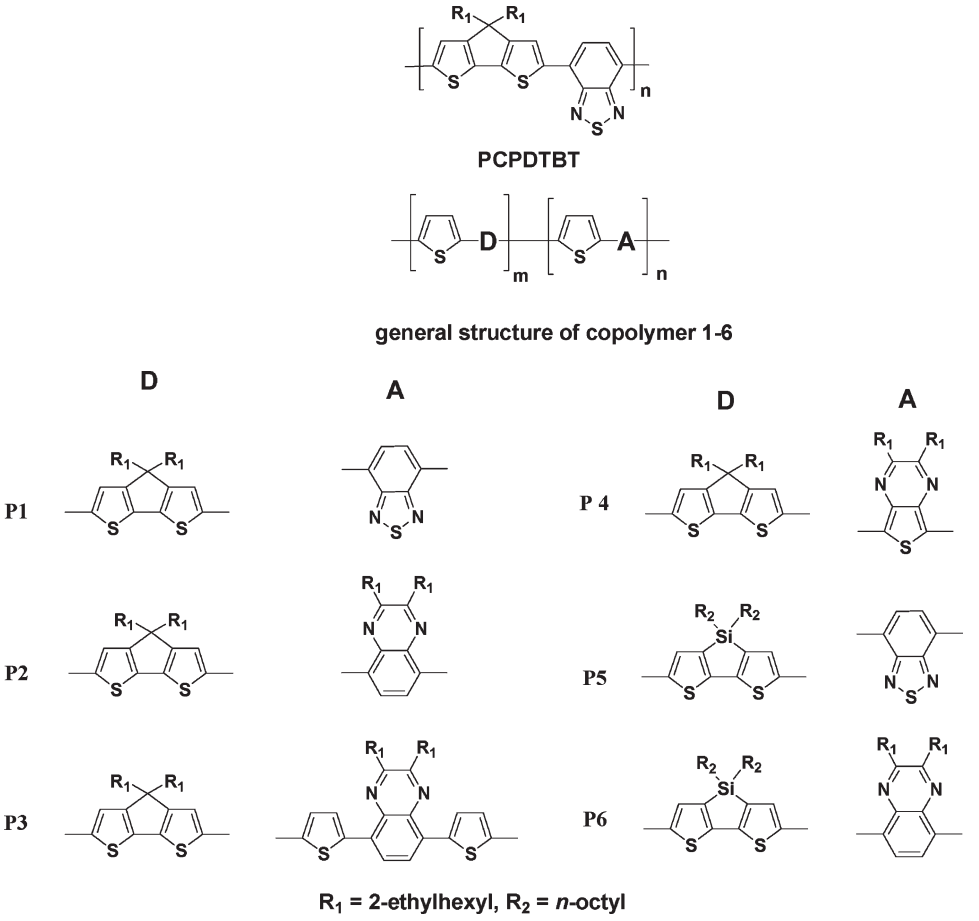

Poly[2,6-(4,4-bis(2-ethylhexyl)-4*H*-cyclopenta[2,1-*b*;3,4-*b*′]dithiophene)-*alt*-4,7-(2,1,3-benzothiadiazole)] (PCPDTBT) using CPDT as the donor and benzothiadiazole (BT) as the acceptor represents one of the most promising LBG polymers for the use in PSCs.[8a] Although such a structurally well-defined alternating D−A copolymer can effectively shift its absorption spectrum to the longer wavelengths in the near-infrared region, the dominating ICT absorption located at ca. 600−800 nm significantly decreases the localized $\pi-\pi^*$ transitions and sacrifices the absorption ability in the visible region from 450 to 600 nm. Furthermore, the high content of acceptor portions which possess high electron affinity may reduce the intrinsic hole mobility of the p-type polymer.[9] To address this issue, one of the effective ways to modulate the optical and electrical properties of low band gap polymers is to make random copolymers by adjusting the donor/acceptor ratios.[10] Herein, we design and synthesize a new three-component random D−A copolymer **P1** where the CPDT donor and the benzothiadiazole acceptor are dispersed and separated by the unsubstituted thiophene spacers in the conjugated backbone (Scheme 1). The incorporation of electron-rich thiophene units in this copolymer not only improves the hole mobility as a result of reducing the concentration of solubilizing groups and increasing the content of hole conductor but also induces more intense electronic transitions in the whole visible range to broaden the absorption bandwidth.[11] Recently, Heeger and co-workers reported a highly efficient tandem cell achieving an efficiency over 6% by utilizing two p-type conjugated polymers in the two independent active layers to effectively harvest the solar photons.[12] The poly(3-hexylthiophene) (P3HT) with a higher band gap to mainly absorb the visible light and the PCPDTBT with a smaller band gap responsible to absorb the near-infrared light were chosen as a suitable pair of absorber. Inspired by this work, we envisioned that simply combining two p-type conjugated polymers which are capable of absorbing light in the complementary wavelength regions in a single active layer would be a practical strategy to maximize the light harvesting. The incorporation of a third component in the active layer has been utilized to improve open-circuit voltage[13] and control morphology[14] in PSCs. Although the panchromatic concept has been sporadically demonstrated by adding porphyrin-based small molecule dyes as the third component,[15] so far using two p-type conjugated polymers has not been exploited due to the problems of immiscibility or phase separation. Regarding the fact that summation of the individual absorption spectra of PCPDTBT and **P1** can produce a markedly wide and strong absorption spectrum covering from 400 to 900 nm and the fact that PCPDTBT and **P1** have compatible polymer structures, the ternary blend system through mixing PCPDTBT and **P1** along with an n-type material of $PC_{71}BM$ in the active layer was investigated.

On the other hand, in order to fine-tune the optical and electrical properties, three-component random polymers **P2**−**P4** were also designed and synthesized in a manner similar to **P1**, except that the quinoxaline (QU) and thienopyrazine (TP) units were employed as the acceptors with different electron-withdrawing strength. Moreover, **P5** and **P6** using the DTS unit as the donor along with benzothiadiazole and quinoxaline moieties as the acceptors were also prepared for comparison (Scheme 1). In this paper, we report the synthesis and characterization of the six aforementioned polymers and their photovoltaic performances in the BHJ polymer solar cells. The structure−properties relationships in these polymers are also discussed in detail.

Scheme 2. Synthesis of Donor Monomer D1

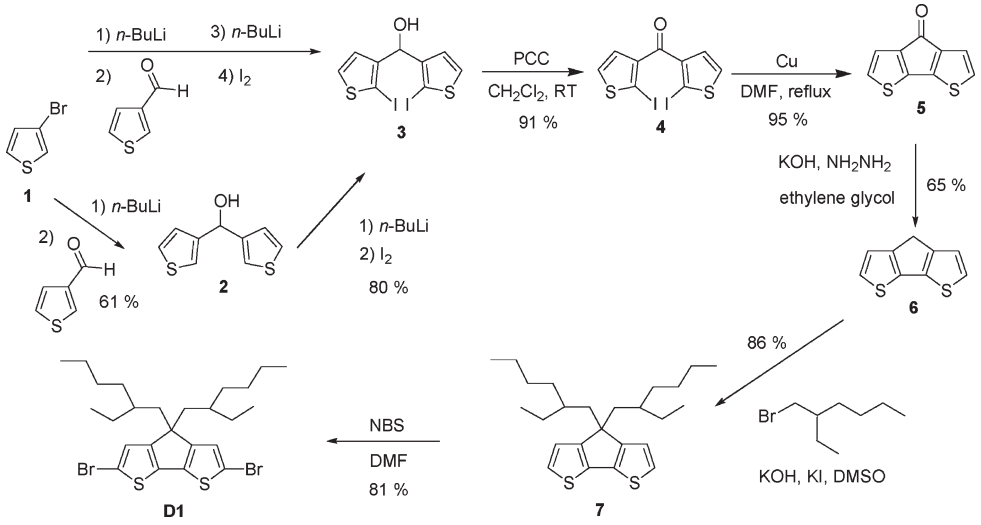

Scheme 3. Synthesis of Donor Monomers D2 and D3

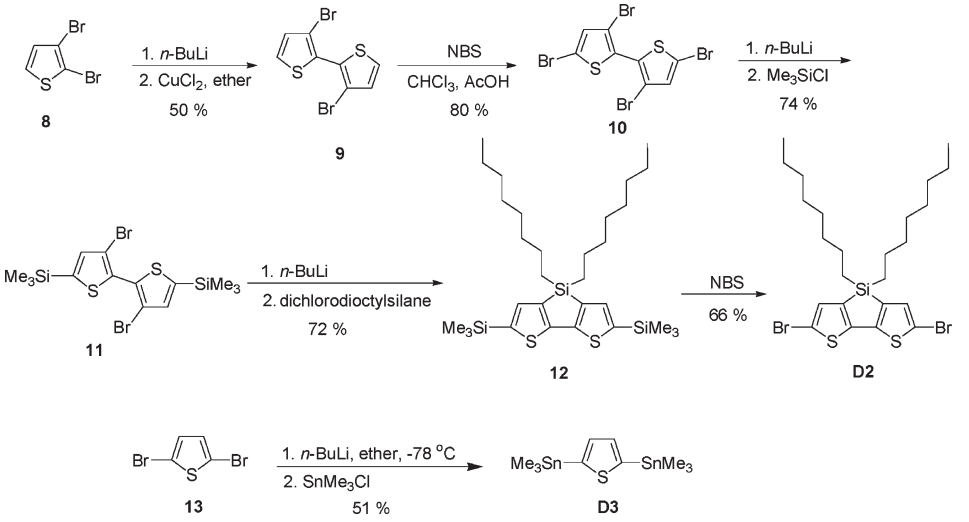

Results and Discussion

Synthesis. A number of synthetic routes directed toward the preparation of useful 4*H*-cyclopenta[2,1-*b*:3,4-*b*′]dithiophene (CPDT) derivatives have been reported and require laborious multistep of synthesis and purification.[16] The key building block leading to CPDT is cyclopentadithiophen-4-one (**5**). Brzeziński et al. described an efficient synthesis of cyclopentadithiophen-4-one via a three-step protocol as shown in the Scheme 2.[17] The key step is the direct synthesis of bis(2-iodothiophen-3-yl)methanol (**3**) from 3-bromothiophene (**1**) through sequential lithiation/nucleophilic addition and lithiation/iodination in one pot. However, the reaction condition seems tedious and not easy to control, always resulting in low chemical yield of compound **3**. We provide here a more practical way based on Brzeziński route where the first step is modified into two separated steps.

Lithiation of 3-bromothiophene with *n*-butyllithium followed by quenching with 3-formylthiophene yielded di(thiophen-3-yl)methanol (**2**). It is noteworthy that the order of addition appears to be very essential. A clean conversion into 3-lithiothiophene can be achieved by slow addition of 3-bromothiophene in ether into a solution of a slight excess of *n*-butyllithium. The formation of undesired but thermodynamically more stable 2-lithiothiophene can be therefore greatly suppressed. The isolated and purified product of compound **2** was lithiated again regioselectively at the 2-position due to the ortho-directing effect, followed by reacting with iodine to furnish compound **3**. PCC oxidation of compound **3** afforded compound **4** which underwent intramolecular cyclization to form **5** by the Ullmann coupling reaction. Ketone **5** was further reduced to **6** by the hydrazine Wolff−Kishner reduction. The methylene proton in **6** is acidic enough to carry out double ethylhexyl alkylation in the presence of potassium hydroxide to obtain **7** which was brominated to monomer **D1** by *N*-bromosuccinimide (NBS) (Scheme 2).

The synthesis of the dithienosiloles **D2** and **D3** is shown in Scheme 3. Lithiation of compound **8** in the presence of copper dichloride resulted in the formation of dimerized compound **9**, which was then brominated to afford compound **10**. By a selective lithium-bromide exchange followed by nucleophilic substitution, the trimethylsilyl group was introduced to the 5,5′-position of the bithiophene compound **11** to act as a protecting group. As a consequence, the subsequent lithiation in compound **11** only occurred at the 3,3′-position of the bithiophene, which then underwent cyclization through double addition to dioctyldichlorosilane to gave **12**. NBS bromination via electrophilic aromatic

Scheme 4. Synthesis of Acceptor Monomers A2−A4

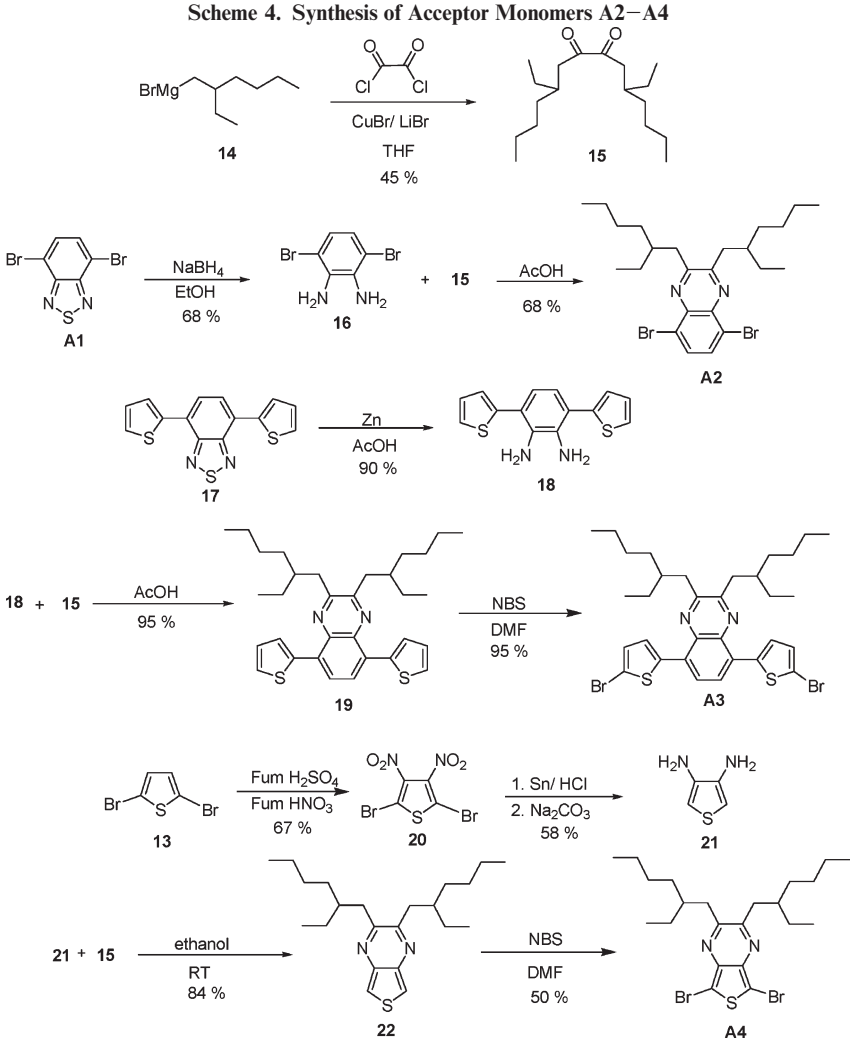

substitution to replace the trimethylsilyl moiety resulted in the formation of compound **D2**. 2,5-Bis(trimethylstannyl)-thiophene (**D3**) was prepared by lithiation of **13** followed by quenching with trimethyltin chloride.

The synthesis of the acceptor monomers **A2**−**A4** are depicted in Scheme 4. In order to ensure the solubility of resulting polymers for solution processability, two branched 2-ethylhexyl groups were introduced to quinoxaline and thienopyrazine acceptors for the first time. The key intermediate 1,2-diketone **15** with two 2-ethylhexyl chains was synthesized by treatment of 2-ethylhexylmagnesium bromide with oxalyl chloride in the presence of CuBr and LiBr. Compound **16** was obtained by $NaBH_4$ reduction of 4,7-dibromobenzothiadiazole (**A1**). Double imine condensation of **16** with **15** led to the formation of quinoxaline **A2**. Monomer of quinoxaline dithiophene **A3** was synthesized by a similar manner starting from compound **17** through the reduction, condensation, and bromination via **18** and **19**.

Nitration of **13** led to the compound **20**, which was debrominated and then reduced to 3,4-diaminothiophene (**21**). In a similar manner, **A4** was synthesized by the imination of **21** and **15**, followed by the NBS bromination. All of the final monomers and their intermediates were fully characterized by ^{1}H NMR and ^{13}C NMR.

As shown in Table 1, 2,5-bis(trimethylstannyl)thiophene (**D3**) was copolymerized with the dibromo donor (**D1** or **D2**) and the dibromo acceptor (**A1** or **A2**−**A4**) to generate the corresponding **P1**−**P6** by the Stille coupling in the presence of $Pd_2(dba)_3$ as the catalyst and tri(*o*-tolyl)phosphine as the ligand. In the preparation of each polymer, the feed molar ratio of **D3** to the corresponding donor and the acceptor monomer in the reaction is 1:0.5:0.5. It is noteworthy that all the polymerization reactions were carried out under microwave-assisted condition in only 45 min to produce the polymers with relatively high number-average molecular weights (M_n) from 19 to 44 kDa.[18] After purification by Soxhlet extraction, a narrow molecular weight distribution with polydispersity index below 2.5 was obtained. (Table 1). Owing to the presence of 2-ethylhexyl or octyl groups in the donor or acceptor units, all the polymers are highly soluble in

Table 1. Comonomers and Molar Ratios Leading to P1−P6 by Stille Coupling and Molecular Weight, PDI, and Thermal Properties of P1−P6

	feed ratio							
copolymer	1	0.5	0.5	M_w[a]	M_n[a]	PDI[a]	T_g (°C)	T_d (°C)[b]
P1	**D3**	**D1**	**A1**	65 000	26 000	2.50	66	396
P2	**D3**	**D1**	**A2**	58 000	27 000	2.15	54	390
P3	**D3**	**D1**	**A3**	38 000	19 000	2.00	51	401
P4	**D3**	**D1**	**A4**	78 000	36 000	2.17	56	367
P5	**D3**	**D2**	**A1**	38 000	22 000	1.73	55	418
P6	**D3**	**D2**	**A2**	97 000	44 000	2.18	52	367

[a] Molecular weights were determined by gel permeation chromatography (GPC) in THF using polystyrene standards. [b] Onset decomposition temperature (5% weight loss) measured by TGA.

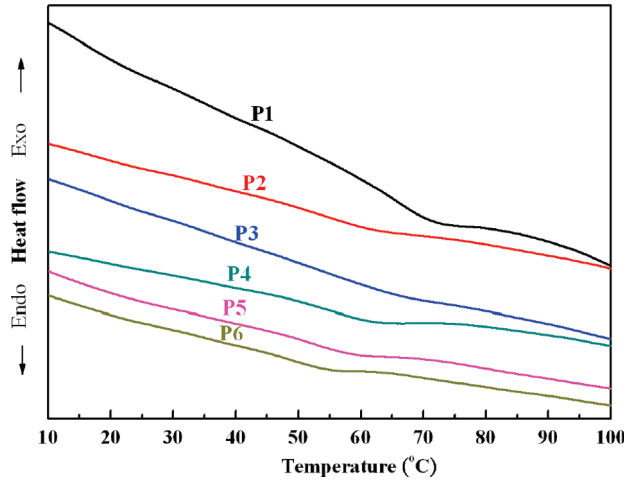

Figure 1. DSC measurements of **P1**−**P6** with a ramping rate of 10 °C/min.

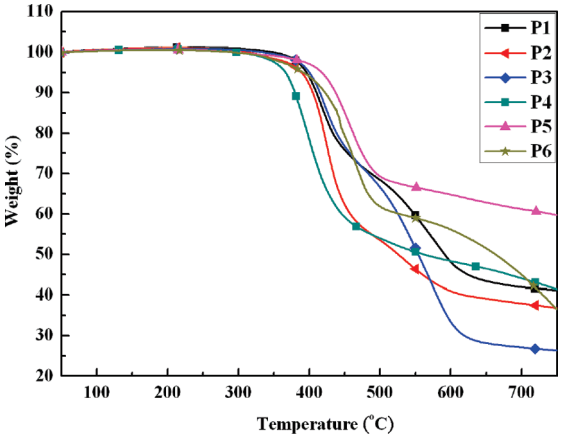

Figure 2. TGA measurements of **P1**−**P6** with a ramping rate of 10 °C/min.

common organic solvents such as chloroform, THF, toluene, and chlorobenzene.

Thermal Properties. Thermal properties of **P1**−**P6** measured by differential scanning calorimetry (DSC) and thermal gravimetric analysis (TGA) are summarized in Table 1. Each polymer shows a glass transition temperature in the range from 51 to 66 °C without the observation of melting point, suggesting that these random copolymers tend to form amorphous glasses (Figure 1). Because of the fact that there is no aliphatic side chain on the benzothiadiazole unit, **P1** has smaller free volume and thus exhibits higher T_g at 65 °C compared to the other CPDT-based polymers with the acceptors functionalized with alkyl chains. The decomposition temperatures (T_d) of these polymers are located from 367 to 418 °C, demonstrating their sufficiently high thermal stability for the applications of PSCs (Figure 2). Notably, the increasing trend of T_d (**P1** > **P2** > **P4**) also implies that thermal stability of the acceptor unit is in the order BT > QU > TP.

Optical and Electrochemical Properties. The UV−vis absorption characteristics of the CPDT- and DTS-based polymers were measured in both dilute toluene solutions (Figure 3) and in spin-coated films (Figure 4) with the relevant optical parameters summarized in Table 2.

For the CPDT-based polymers, **P4** exhibits the most red-shifted absorption maximum (λ_{max}) in solution at 710 nm followed by **P1** at 613 nm, **P2** at 571 nm, and **P3** at 550 nm.

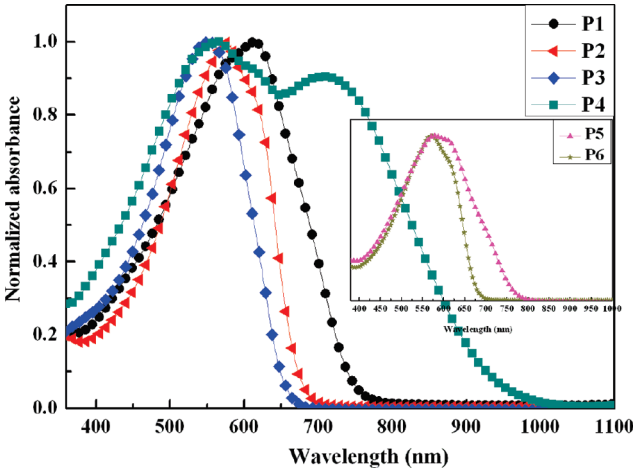

Figure 3. Normalized absorption spectra of **P1**−**P6** in toluene solution.

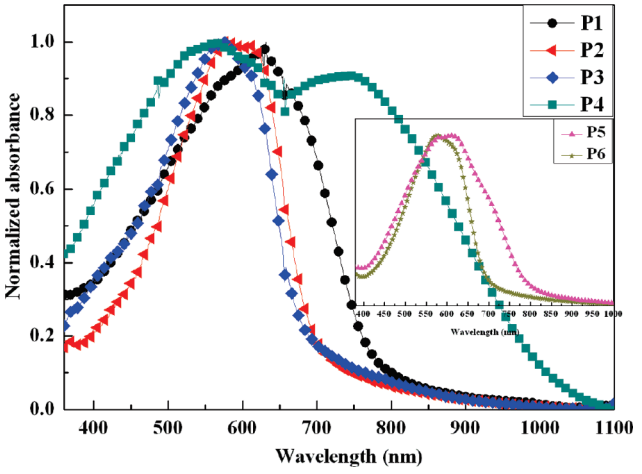

Figure 4. Normalized absorption spectra of **P1**−**P6** in solid state.

Compared with the D−A alternating PCPDTBT polymer, random copolymer **P1**, which contains more thiophene units and less BT content, shows a blue-shifted but broader absorption spectrum covering the whole UV−vis region. This is evidenced by the larger full width at half-maximum (fwhm) of **P1** (264 nm) than that of PCPDTBT (219 nm) in the solid-state absorption spectra. The optical band-gaps (E_g^{opt}) deduced from the absorption edges of thin film spectra are in the following order: **P3** (1.82 eV) > **P2** (1.77 eV) > **P1** (1.59 eV) > **P4** (1.20 eV). Because **P1**−**P4** have the similar molecular composition except for the acceptor units, the difference of their λ_{max} as well as E_g^{opt} apparently points out that the acceptor strength is in the order TP > BT > QU.

It is known that the HOMO−LUMO band gap decreases linearly as a function of the increasing quinoid character of a given conjugated polymer.[19] As a result, the acceptor that induces more quinoid population in the polymer main chain will have stronger band gap lowering ability. As illustrated in Scheme 5, the increasing degree of the quinoid character of these acceptors is shown in the order TP > BT > QU. Because pyrazine has a larger aromatic resonance energy than thiophene, the thienopyrazine unit in the conjugated main chain tend to favorably adopt the quinoid form through π-electron delocalization in order to selectively preserve the pyrazine's aromaticity. This in turn decreases the bond length alternation and greatly reduces the band gap of **P4** to 1.2 eV.[20] Consequently, TP unit exerts the most

Table 2. Optical and Electrochemical Properties of P1−P6

	toluene solution			thin film						
polymer	λ_{max} (nm)	λ_{onset} (nm)	E_g^{opt} (eV)	λ_{max} (nm)	λ_{onset} (nm)	E_g^{opt} (eV)	E_{ox}^{onset} (V)	HOMO[a] (eV)	LUMO[b] (eV)	$\lambda_{max,film} - \lambda_{max,solution}$ (nm)
P1	613	753	1.65	631	780	1.59	0.37	−5.17	−3.58	18
P2	571	687	1.80	579	699	1.77	0.25	−5.05	−3.28	8
P3	550	664	1.87	576	683	1.82	0.33	−5.13	−3.31	26
P4	566, 710	965	1.28	569, 741	1030	1.20	0.22	−5.02	−3.82	31
P5	579	772	1.61	611	790	1.57	0.35	−5.15	−3.58	32
P6	571	677	1.83	578	692	1.79	0.27	−5.07	−3.28	8

[a] The HOMO energy levels were obtained from the equation HOMO = $-4.8 - E_{ox}^{onset}$. [b] LUMO levels of **P1**−**P6** were obtained from the equation LUMO = HOMO + E_g^{opt}.

Scheme 5. Aromatic and Quinoid Form of Thienopyrazine, Benzothiadiazole, and Quinoxaline Units

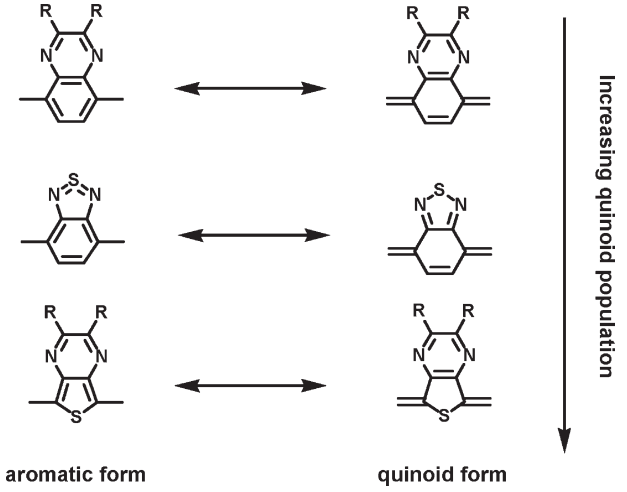

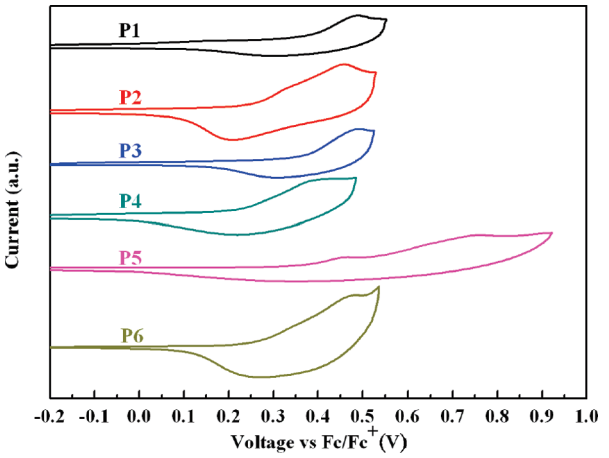

Figure 5. Cyclic voltammograms of **P1**−**P6** in thin film at a scan rate of 80 mV/s.

powerful impact on lowering the band gap when incorporated into the conjugated polymer. In addition to containing hypervalent sulfur to withdrawing electron,[21] benzothiadiazole unit also has a great deal of quinoid population because more stable classical 1,2,5-thiadizole rings are generated in this form.[22] Increasing the quinoidization population in the conjugated polymer will accompany an increase of the backbone planarization which induces strong interchain $\pi-\pi$ interactions in the film state. Therefore, it is reasonable to see that **P4** shows the largest 31 nm λ_{max} red shift from solution to solid state, compared to 18 nm for **P1** and 8 nm for **P2**. In addition, **P4** exhibits two distinct absorption bands with almost equal intensity. These two peaks cover extremely broad region from UV through visible to NIR regions (300 to 1000 nm). The lower energy band could be attributed to the ICT, while locally conjugated transitions are responsible for the higher energy band. The other polymers with weaker acceptors actually also have ICT bands. However, they are located at shorter wavelengths and overlapped with the localized π-π* transition band so that only a very broad band was observed. With two additional thiophene rings attached at the quinoxaline unit to decrease the degree of ICT, **P3** shows a slightly blue-shifted absorption spectrum and thus higher band gap in comparison with **P2**. Cyclic voltammetry (CV) was employed to examine the electrochemical properties and evaluate the HOMO levels of the polymers (Table 2 and Figure 5).

The HOMO energy levels of these polymers are between −5.17 and −5.02 eV with small variation, which shows that the HOMO level is more dependent on the electron-rich donors in the polymer. The LUMO energy levels were approximately estimated by subtracting the band gap values from the corresponding HOMO levels. The influence of the electron acceptors on the absorption charge transfer band (λ_{max}: **P4** > **P1** > **P2** and **P5** > **P6**) totally reflects the position of LUMO levels (LUMO: **P4** > **P1** > **P2** and **P5** > **P6**), indicating that the LUMO energy levels are mainly determined by the electron acceptors. Apparently, the more powerful the acceptor, the higher the electron affinity, which finally leads to lower-lying LUMO level in these polymers. It should be noted that **P1** and **P2** show very similar optical and electrochemical properties with **P5** and **P6**, respectively, which suggests that both the bridged bithiophene units, CPDT and DTS, have very similar steric and electronic effects on the polymers. Figure 6 shows the energy diagram for the HOMO−LUMO levels of **P1**−**P6**.

Hole Mobility and Photovoltaic Characteristics. Hole-only devices (ITO/PEDOT:PSS/polymer/Au) were fabricated in order to estimate the hole mobilities of these polymers including PCPDTBT via space-charge limit current (SCLC) theory. Bulk heterojunction photovoltaic cells were also fabricated on the basis of ITO/PEDOT:PSS/polymer:$PC_{71}BM$/Ca/Al configuration, and their performances were measured under 100 mW/cm^2 AM1.5 illumination. $PC_{71}BM$ was used due to its stronger light absorption in the visible region than that of $PC_{61}BM$.[23] The characterization data are summarized in Table 3, and the $J-V$ curves of these polymers are shown in Figure 7. The devices based on **P1** and **P5** with benzothiadiazole unit as the acceptor exhibit the highest PCE of 2.0% and 2.2%, respectively. While using PCPDTBT as the p-type material, the device showed a lower PCE of 1.4% under the same fabrication conditions. The better photovoltaic performance of **P1** and **P5** over PCPDTBT might be ascribed to their slightly enhanced hole mobilities and broader absorption band widths in visible region. **P2** and **P6** with quinoxaline moiety as the acceptor show relatively lower hole mobilities of 9.5×10^{-5} and

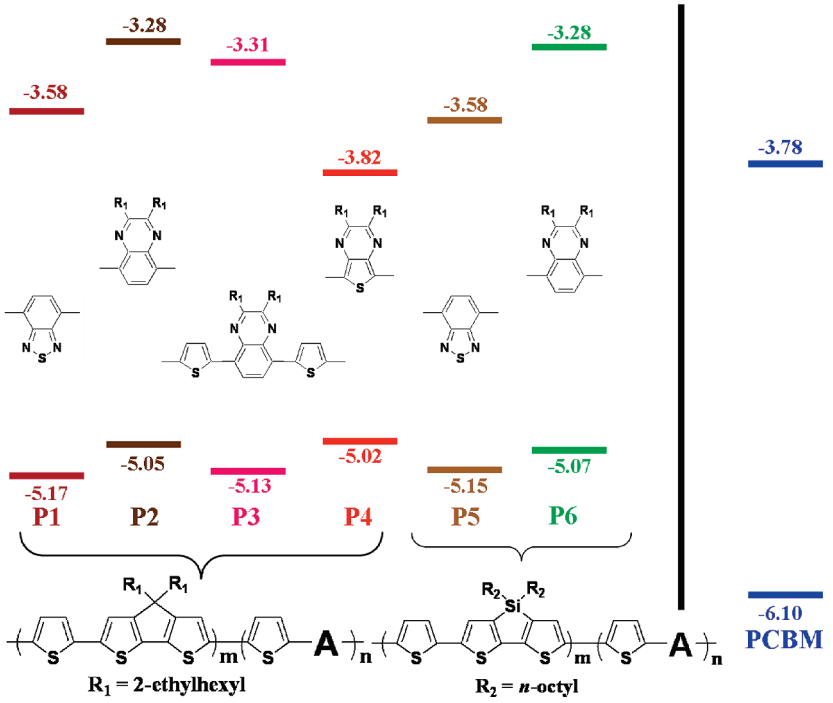

Figure 6. Energy diagram of HOMO−LUMO levels for **P1**−**P6** and PCBM.

Table 3. Photovoltaic Characteristics of P1−P6 and Ternary Blend Systems[a]

copolymer	wt % ratio of polymer and $PC_{71}BM$	μ_h[b] ($cm^2/(V\ s)$)	V_{oc} (V)	J_{sc} (mA/cm^2)	FF (%)	PCE[c] (%)
P1	1:2	1.8×10^{-4}	0.58	9.8	36	2.0 (±0.10)
P2	1:1	9.5×10^{-5}	0.62	1.4	33	0.3 (±0.03)
P3	1:1	1.8×10^{-4}	0.63	2.1	41	0.7 (±0.10)
P4	1:1	7.7×10^{-4}	0.44	3.5	38	0.6 (±0.05)
P5	1:2	1.7×10^{-4}	0.51	9.6	45	2.2 (±0.06)
P6	1:1	2.3×10^{-5}	0.64	1.1	40	0.3 (±0.05)
PCPDTBT	1:2	1.4×10^{-4}	0.65	6.3	34	1.4 (±0.12)
PCPDTBT/P3HT	1:1:4		0.70	4.1	34	1.0 (±0.05)
PCPDTBT/**P1**	1:1:4		0.64	11.1	36	2.5(±0.26)
PCPDTBT/**P5**	1:1:4		0.54	9.5	37	1.9 (±0.14)

[a] All the performance parameters were averaged over four devices. [b] Determined by space-charge limit current (SCLC) theory. [c] Standard deviation is shown in the parentheses.

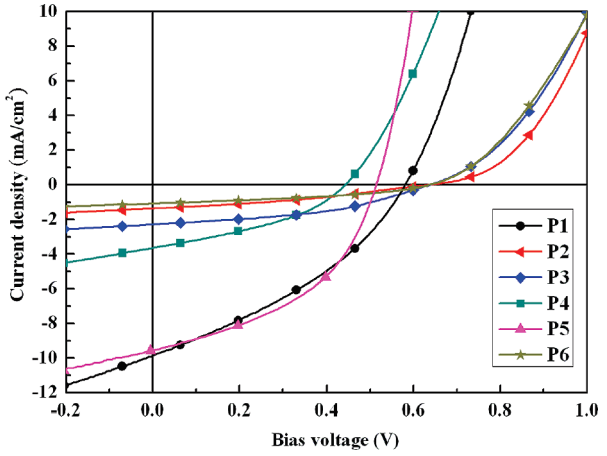

Figure 7. $J-V$ characteristics of ITO/PEDOT:PSS/polymer:$PC_{71}BM$/Ca/Al under illumination of AM1.5 at 100 mW/cm^2.

2.3×10^{-5} $cm^2/(V\ s)$, respectively, which results in a low J_{sc} of 1.4 mA/cm^2 for **P2** and 1.1 mA/cm^2 for **P6** as well as smaller PCEs of 0.3%. Compared to **P2**, the introduction of two thiophenes into the quinoxaline unit in **P3** increases the intrinsic hole mobility to 1.8×10^{-4} $cm^2/(V\ s)$ and J_{sc} to 2.1 mA/cm^2. As a result, PCE is also improved to 0.7% in the device. Although **P4** shows the highest hole mobility of 7.7×10^{-4} $cm^2/(V\ s)$ and broadest absorption spectrum, the device only resulted in a low PCE of 0.6%. This indicates that the strong electron-accepting ability of the thienopyrazine unit leads to a lower LUMO level in **P4**, which prohibits favorable electron transfer from **P4** to $PC_{71}BM$. Indeed, the LUMO level of **P4** is determined to be −3.82 eV, which is even lower than −3.78 eV reported for $PC_{61}BM$.[24] It should be noted the LUMO of $PC_{71}BM$ is very close to that of $PC_{61}BM$.[25] We expected that the device performance based on **P4** can be improved if an n-type material with a LUMO level below −4.0 eV is utilized.

Ternary Blend in Active Layer. Although **P1** and PCPDTBT represent the best two CPDT-based polymers in the study, further improvement of these materials to achieve higher device performance is desirable. As far as optical properties are concerned, the PCPDTBT lacks of absorption in the visible range while **P1** is short of absorption in the NIR region. To circumvent the UV−vis and NIR absorption trade-off that is always encountered in a single p-type material, the most straightforward and easiest strategy is to blend two p-type polymers and an n-type material to effectively harvest the light. A BHJ device with an active

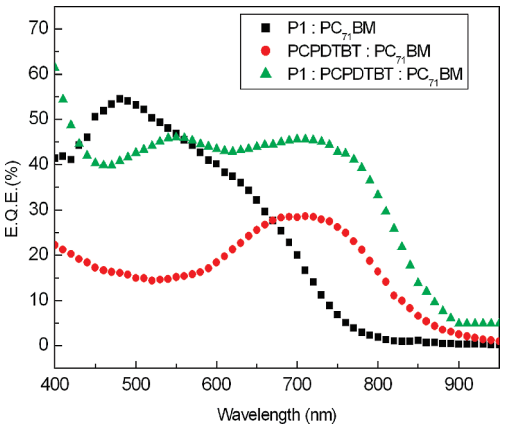

Figure 8. IPCE spectrum of binary blend of PCPDTBT/$PC_{71}BM$ (1:2, w/w) and **P1**/$PC_{71}BM$ (1:2, w/w) as well as ternary blend of PCPDTBT/**P1**/$PC_{71}BM$ (1:1:4, w/w/w).

layer containing the ternary blend of PCPDTBT/**P1**/$PC_{71}BM$ (1:1:4 in wt %) was therefore fabricated and investigated.

As expected, this device reached the best performance, showing a V_{oc} of 0.64 V, a J_{sc} of 11.1 mA/cm^2, a FF of 36%, and a PCE of 2.5%, which outperforms the devices based on the binary blending systems of PCPDTBT/$PC_{71}BM$ (1:2 in wt %) or **P1**/$PC_{71}BM$ (1:2 in wt %) under the identical fabrication and measurement conditions. As shown in Figure 8, the IPCE spectrum of the ternary blend device is essentially the result of summation of the two individual spectra from PCPDTBT and **P1**-based devices, covering from 400 to 800 nm with the external quantum efficiency over 40%. To the best of our knowledge, this is the first time that using two p-type conjugated polymers with complementary absorption ability within a single active layer to improve the solar cell performance has been demonstrated. Concerning that the PCPDTBT/P3HT pair is also able to provide complementary absorption spectra, we fabricated a device using PCPDTBT/P3HT/$PC_{71}BM$ (1:1:4 in wt %) as the ternary blend system for comparison. Unfortunately, this device only produced a V_{oc} of 0.70 V, a J_{sc} of 4.1 mA/cm^2, a FF of 34%, and an overall lower PCE of 1%. These results reveal that, in addition to the prerequisite of complementary absorption coverage, compatibility between two conjugated polymers plays an important role to maintain the original bulk morphology for efficient exciton dissociation and charge transport. Figure 9 shows the diffractograms of P3HT/$PC_{71}BM$ and P3HT/PCPDTBT/$PC_{71}BM$ composite films. It is found that the binary P3HT/$PC_{71}BM$ blend exhibits a strong peak at $2\theta = 5.4°$, which is a typical observation assigned for the P3HT crystallites with *a*-axis orientation.[26] However, this peak intensity is significantly reduced in the ternary blend of P3HT/PCPDTBT/$PC_{71}BM$. This result indicates that the degree of crystallinity of P3HT is dramatically attenuated when PCPDTBT with more amorphous character is physically blended into the active layer. The XRD measurement of binary **P1**/$PC_{71}BM$ and ternary **P1**/PCPDTBT/$PC_{71}BM$ blends was also carried out, showing very similar result with no apparent peaks in the XRD due to their amorphous nature (Figure 9). Both PCPDTBT and **P1**, which are comprised of thiophene and benzothiadiazole units, have very similar structural composition and thus superior compatibility. As a result, the morphology of the active layer can be retained while the absorption ability is greatly enhanced. It is noteworthy that a solar cell device containing ternary blend system

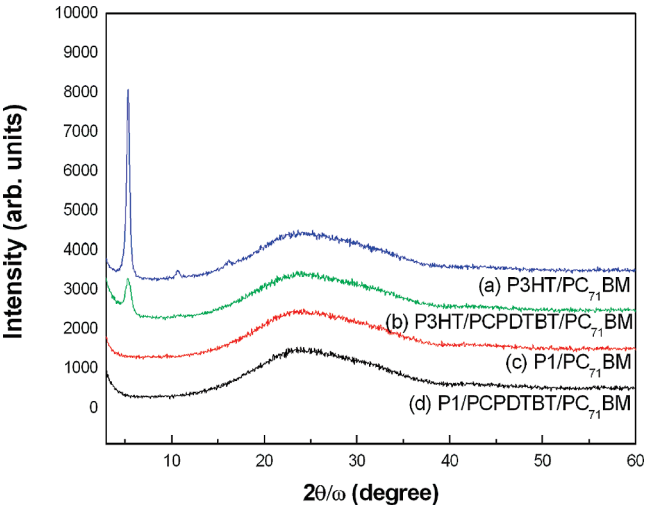

Figure 9. XRD patterns of (a) P3HT/$PC_{71}BM$, (b) P3HT/PCPDTBT/$PC_{71}BM$, (c) **P1**/$PC_{71}BM$, and (d) **P1**/PCPDTBT/$PC_{71}BM$ composite films deposited on ITO/PEDOT:PSS substrates. Curves are offset for clarity.

P5/PCPDTBT/$PC_{71}BM$ was also fabricated for comparison. The device performance of **P5**/PCPDTBT/$PC_{71}BM$ with a PCE of 1.9% is worse than that of **P1**/PCPDTBT/$PC_{71}BM$ system under identical fabrication conditions. Very recently, Yang et al. reported that by simply replacing the 5-position carbon of PCPDTBT with a silicon atom to form a polymer PSBTBT, the polymer changes from an amorphous (PCPDTBT) to a highly crystalline structure (PSBTBT), leading to very different polymer packing properties.[27] Concerning that **P1** and PCPDTBT have the same donating CPDT segment whereas **P5** uses the DTS unit as the donor, **P1** should presumably have better compatibility with PCPDTBT than **P5** in the solid state. This difference may explain why **P1**/PCPDTBT/$PC_{71}BM$ is better than the **P5**/PCPDTBT/$PC_{71}BM$ system, although **P5** shows better device performance than **P1** in the binary system. The relevant research utilizing the ternary blend concept and the optimization condition are currently underway.

Conclusions

We have successfully designed and synthesized six highly soluble donor−acceptor random copolymers **P1**−**P6**, symbolized as (thiophene donor)$_m$−(thiophene acceptor)$_n$, in which equal molar amounts of donor (CPDT or DTS) and acceptor monomers (BT, TP, QU, or DTQU) were copolymerized with unsubstituted thiophene units by the Stille coupling. A modified route to improve the synthesis of the useful CPDT monomer was also presented. The ability of the acceptor to induce the planar quinoid form in the conjugated polymers is found to follow the trend TP > BT > QU, which consistently determines the trend of the relevant optical and electrical properties. (i.e., λ_{max}: **P4** > **P1** > **P2**; E_g^{opt}: **P4** < **P1** < **P2**; mobility: **P4** > **P1** > **P2**). From the comparison of **P1** with **P5** as well as **P2** with **P6**, it is shown that the two bridged bithiophenes, DTS and CPDT, have very similar structural and electronic effects on the polymers. Compared to the alternating PCPDTBT analogue, random copolymer **P1**, containing higher thiophene and lower BT contents, shows more blue-shifted but broader absorption spectra, higher hole mobility, leading to a higher PCE of 2.0%. Regarding that **P1** shows a higher band gap with strong absorption in visible region and PCPDTBT has a lower band gap to mainly absorb NIR light, a BHJ device with the active layer containing ternary blend of PCPDTBT/**P1**/$PC_{71}BM$ was investigated. This device achieved

an enhanced PCE of 2.5%, which outperforms the devices based on the binary blending systems of PCPDTBT/$PC_{71}BM$ (PCE = 1.4%) or **P1**/$PC_{71}BM$ (PCE = 2.0%) under identical conditions. Such an improvement is attributed to the combination of complementary absorption and compatible structure of the **P1** and PCPDTBT polymers. It is envisioned that using two compatible conjugated polymers to form a ternary blend in the active layer will provide a new direction for effectively enhancing the light absorption ability and solar cell performance.

Experimental Section

General Measurement and Characterization. All chemicals are purchased from Aldrich or Acros and used as received unless otherwise specified. ^1H and ^{13}C NMR spectra were measured using Varian 300 MHz instrument spectrometer. A differential scanning calorimeter (DSC) was measured on TA Q200 Instrument, and TGA was recorded on Perkin-Elmer Pyris under a nitrogen atmosphere at a heating rate of 10 °C/min. Absorption spectra were taken on a HP8453 UV−vis spectrophotometer. The molecular weight of polymers was measured by gel permeation chromatography (Viscotek VE2001GPC) using a Waters Styragel column (concentration: 1 mg/1 mL in THF; flow rate: 1 mL/1 min), and polystyrene was used as the standard (THF as the eluent). FT-IR spectra were taken on a Perkin-Elmer spectrophotometer by using KBr pellets. The electrochemical cyclic voltammetry was conducted on a Bioanalytical Systems Inc. analyzer. A carbon glass coated with a thin polymer film was used as the working electrode and an Ag/AgCl as the reference electrode, while 0.1 M tetrabutylammonium hexafluorophosphate ($TBAPF_6$) in acetonitrile was the electrolyte. CV curves were calibrated using ferrocene as the standard, whose HOMO is set at −4.8 eV with respect to zero vacuum level.

Fabrication and Characterization of BHJ Devices. ITO/glass substrates were ultrasonically cleaned sequentially in detergent, water, acetone, and IPA. Then, the substrates were covered by a 30 nm thick layer of PEDOT:PSS (Clevios P provided by H.C. Stark) by spin-coating. After annealing in air at 200 °C for 10 min, the samples were cooled down to room temperature. Polymers were dissolved in *o*-dichlorobenzene (ODCB) (1.0 wt %), and $PC_{71}BM$ (purchased from Nano-C) was added to reach the desired ratio. The solution was then heated at 70 °C for 1 h and stirred overnight at room temperature. Prior to deposition, the solution was filtrated through a 0.45 μm filter, and the substrate was transferred in a glovebox. The photoactive layer was then spin-coated at different spin-coating speed in order to tune its thickness. After drying, the samples were annealed (110−140 °C) for 15 min. The detailed processing parameters (spin-coating speed; annealing temperature) are shown as follows: **P1**/$PC_{71}BM$ (600 rpm; 110 °C), **P2**/$PC_{71}BM$ (1000 rpm; 140 °C), **P3**/$PC_{71}BM$ (1000 rpm; 140 °C), **P4**/$PC_{71}BM$ (1000 rpm; 110 °C), **P5**/$PC_{71}BM$ (1500 rpm; 110 °C), **P6**/$PC_{71}BM$ (1000 rpm; 140 °C), **P1**/PCPDTBT/$PC_{71}BM$ (1200 rpm; 110 °C), **P5**/PCPDTBT/$PC_{71}BM$ (1200 rpm; 110 °C), P3HT/PCPDTBT/$PC_{71}BM$ (1200 rpm; 140 °C). The cathode made of calcium (35 nm thick) and aluminum (100 nm thick) was evaporated through a shadow mask under high vacuum ($<10^{-6}$ Torr). Finally, the devices were encapsulated, and $I-V$ curves were measured in air. Each device is constituted of 4 pixels defined by an active area of 0.04 cm^2. Finally, the devices were encapsulated, and $I-V$ curves were measured in air.

Electrical Characterization under Illumination. The devices were characterized under 100 mW/cm^2 AM1.5 simulated light measurement (Yamashita Denso solar simulator). Current−voltage ($J-V$) characteristics of PSC devices were obtained by a Keithley 2440 SMU. Solar illumination conforming the JIS Class AAA was provided by a SAN-EI 300 W solar simulator equipped with an AM1.5G filter. The light intensity was calibrated with a Hamamatsu S1336-5BK silicon photodiode. The performances presented here are the average of the 4 pixels of each device.

Hole-Only Devices. In order to investigate the respective hole mobility of the different copolymer films, unipolar devices have been prepared following the same procedure, except that the active layer is made of pure polymer and the Ca/Al cathode is replaced by evaporated gold (40 nm).

IPCE Measurements. The set of IPCE measurement system and test program were all built up by Optosolar Inc. A 300 W Xe arc light source is coupled to a monochromator to create the scanning light. The lock-in amplifier comes with a built-in chopper controller, which is used to detect and measure very small ac signals accurately, for lock-in measurement with a calibrated Si detector over the 350−1160 nm range. The short-circuit current density of the cell is therefore measured by a lock-in amplifier in the monochromatic incident light under a chopper with a frequency of 50−60 Hz.

Di(thiophen-3-yl)methanol (2). To a 2.5 M solution of *n*-BuLi (27 mL in hexane, 67.5 mmol) in dry ether (40 mL) was added 3-bromothiophene **1** (10 g, 61.3 mmol) dropwise at −78 °C. The resulting mixture was stirred for 30 min at −78 °C. Thiophene-3-carboxaldehyde (5.9 mL, 67 mmol) was added to the mixture solution dropwise. The mixture was allowed to warm up to room temperature and then stirred for 12 h. The reaction solution was extracted with EA (400 mL × 3) and water (200 mL). The combined organic layer was dried over $MgSO_4$. After removal the solvent under reduced pressure, the residue was purified by column chromatography on silica gel (hexane/ethyl acetate, v/v, 15/1) to give a white powder **2** (7.32 g, 61%); mp 62 °C. ^1H NMR ($CDCl_3$, 300 MHz): δ 2.31−2.39 (m, 1 H), 5.93 (d, J = 3.6 Hz, 1 H), 7.03 (dd, J_1 = 5.1, J_2 = 1.2 Hz, 2 H,), 7.18−7.22 (m, 2 H), 7.29 (dd, J_1 = 5.1, J_2 = 3.0 Hz, 2 H). ^{13}C NMR ($CDCl_3$, 75 MHz): δ 69.0, 121.7, 126.2, 126.3, 144.8. MS (EI, $C_9H_8OS_2$): calcd, 196.3; found, 196.

Bis(2-iodothiophen-3-yl)methanol (3). To a solution of **2** (10 g, 50.9 mmol) in dry ether (50 mL) was added a 2.5 M solution of *n*-BuLi in hexane (62.5 mL, 156.3 mmol) dropwise at −78 °C. After stirring at −78 °C for 30 min, a solution of iodine (42.7 g, 168.2 mmol) in dry ether (300 mL) was added into above solution dropwise. The solution was allowed to warm up to room temperature and stirred for 1 h. The aqueous solution of sodium thiosulfate (200 mL) was added, and the two layers were separated. The combined organic layer was dried over $MgSO_4$. After removal the solvent under reduced pressure, the residue was purified by column chromatography on silica gel (hexane/ethyl acetate, v/v, 15/1) to give a cream-colored crystal **3** (18.24 g, 80%); mp 115−117 °C. ^1H NMR ($CDCl_3$, 300 MHz): δ 2.35 (d, J = 3.0 Hz, 1 H), 5.76 (d, J = 3.0 Hz, 1 H), 6.93 (d, J = 5.4 Hz, 2 H), 7.43 (d, J = 5.4 Hz, 2 H). ^{13}C NMR ($CDCl_3$, 75 MHz): δ 71.7, 75.3, 126.9, 131.4, 146.6. MS (EI, $C_9H_6I_2OS_2$): calcd, 448.1; found, 448.

Bis(2-iodo-3-thienyl) Ketone (4). To a stirred solution of **19** (10.04 g, 22 mmol) in dichloromethane (230 mL) was added pyridinium chlorochromate (7.25 g, 34 mmol) in one portion. The mixture solution was stirred at room temperature for 12 h. The solution was extracted with dichloromethane three times (300 mL × 3). The combined organic layer was dried over $MgSO_4$. After removal the solvent under reduced pressure, the residue was purified by column chromatography on silica gel (hexane/ethyl acetate, v/v, 30/1) to give a yellow crystal **4** (9.1 g, 91%); mp 97−99 °C. ^1H NMR ($CDCl_3$, 300 MHz): δ 7.05 (d, J = 5.4 Hz, 2 H), 7.47 (d, J = 5.4 Hz, 2 H). ^{13}C NMR ($CDCl_3$, 75 MHz): δ 81.3, 130.0, 131.6, 143.1, 185.5. MS (EI, $C_9H_4I_2OS_2$): calcd, 446.1; found, 446.

4*H*-Cyclopenta[2,1-*b*:3,4-*b*′]dithiophen-4-one (5). To a stirred solution of **20** (9.1 g, 20 mmol) in DMF (62 mL) was added Cu powder (3.9 g, 60 mmol) in one portion at room temperature, and the mixture solution was refluxed for 15 h. After cooling to room temperature, the solid was filtered off. The filtrate was extracted with water three times (150 mL × 3). The combined

organic layer was dried over $MgSO_4$. After removal the solvent under reduced pressure, the residue was purified by column chromatography on silica gel (hexane/ethyl acetate, v/v, 20/1) to give a dark-red crystal **5** (3.7 g, 95%); mp 136−137 °C. ^{1}H NMR ($CDCl_3$, 300 MHz): δ 6.99 (d, J = 4.8 Hz, 2 H), 7.04 (d, J = 4.8 Hz, 2 H). ^{13}C NMR ($CDCl_3$, 75 MHz): δ 121.7, 127.1, 142.4, 149.2, 182.7. MS (EI, $C_9H_4OS_2$): calcd, 192.3; found, 192.

4*H*-Cyclopenta[2,1-*b*:3,4-*b*′]dithiophene (6). To a suspension solution of **6** (4.31 g, 22.4 mmol) in ethylene glycol (96 mL) was added potassium hydroxide (4.31 g, 76.8 mmol) under a nitrogen atmosphere. The slurry solution was heated to 180 °C, and hydrazine monohydrate (8.6 mL, 177.3 mmol) was added by syringe dropwise. The mixture was stirred at 180 °C for 8 h. The mixture solution was then cooled to room temperature and extracted with ether (250 mL × 3) and water (100 mL). The combined organic layer was dried over $MgSO_4$. After removal of the solvent under reduced pressure, the residue was purified by column chromatography on silica gel (hexane) to give a white crystal **6** (2.60 g, 65%); mp 136−137 °C. ^{1}H NMR ($CDCl_3$, 300 MHz): δ 7.09 (d, J = 4.8 Hz, 2 H), 7.18 (d, J = 4.8 Hz, 2 H). ^{13}C NMR ($CDCl_3$, 75 MHz): δ 31.8, 122.9, 124.4, 138.6, 149.6. MS (EI, $C_9H_6S_2$): calcd, 178.3; found, 178.

4,4-Diethylhexylcyclopenta[2,1-*b*:3,4-*b*′]dithiophene (7). To a suspension solution of **6** (1.55 g, 8.7 mmol), 2-ethylhexyl bromide (3.4 g, 17.4 mmol), and potassium iodide (20 mg) in DMSO (30 mL) was added potassium hydroxide (1.55 g, 27.6 mmol) in one portion at 0 °C. The resulting solution was stirred for 16 h at room temperature and then was extracted with ether (150 mL × 3) and water (50 mL). The combined organic layer was dried over $MgSO_4$. After removal the solvent under reduced pressure, the residue was purified by column chromatography on silica gel (hexane) to give a pale yellow oil **7** (3.0 g, 86%). ^{1}H NMR ($CDCl_3$, 300 MHz): δ 0.58 (t, J = 7.2 Hz, 6 H), 0.75 (t, J = 8.8 Hz, 6 H), 0.78−1.00 (m, 18 H), 1.78−1.88 (m, 4 H), 6.91−6.92 (m, 2 H), 7.10 (d, J = 5.1 Hz, 2 H). ^{13}C NMR ($CDCl_3$, 75 MHz): δ 10.6, 14.1, 22.7, 27.2, 28.6, 34.1, 35.0, 43.2, 53.2, 122.3, 123.9, 136.8, 157.6. MS (EI, $C_{25}H_{38}S_2$): calcd, 402.7; found, 403.

2,6-Dibromo-4,4-diethylhexyl-cyclopenta[2,1-*b*:3,4-*b*′]dithiophene (D1). Under nitrogen, to a solution of **7** (1.5 g, 3.7 mmol) in DMF (37.5 mL) was added *N*-bromosuccinimide (1.33 g, 7.45 mmol) in the dark. The resulting solution was stirred for 12 h at room temperature under nitrogen and then was extracted with ether (150 mL × 3) and water (50 mL). The combined organic layer was dried over $MgSO_4$. After removal the solvent under reduced pressure, the residue was purified by column chromatography on silica gel (hexane) to give a pale yellow oil **D1** (1.7 g, 81%). ^{1}H NMR ($CDCl_3$, 300 MHz): 0.60 (t, J = 6.9 Hz, 6 H), 0.78 (t, J = 6.9 Hz, 6 H), 0.82−1.09 (m, 18 H), 1.74−1.86 (m, 4 H), 6.92−6.94 (m, 2 H). ^{13}C NMR ($CDCl_3$, 75 MHz): δ 10.6, 14.0, 22.7, 27.3, 28.5, 34.0, 35.1, 43.0, 54.9, 110.7, 125.2, 136.6, 155.5. MS (EI, $C_{25}H_{36}Br_2S_2$): calcd, 560.5; found, 560. Elemental analysis (%) Calcd for $C_{25}H_{36}Br_2S_2$: C, 53.57; H, 6.47; Found: C, 54.57; H, 6.44.

3,3′-Dibromo-2,2′-bithiophene (9). To a solution of 2,3-dibromothiophene **8** (12.73 g, 53 mmol) in dry ether (320 mL) was added a 2.5 M solution of *n*-BuLi in hexane (22 mL, 55 mmol) dropwise at −78 °C. After stirring at −78 °C for 1 h, $CuCl_2$ (10.69 g, 79 mmol) was introduced to the solution in one portion. The reaction mixture was stirred at −78 °C for 2 h and then at room temperature for 2 days. The reaction mixture was quenched by 5 M HCl (500 mL) at 0 °C and then extracted with chloroform three times (450 mL × 3). The organic layer was dried over $MgSO_4$. After removal the solvent under reduced pressure, the residue was purified by column chromatography on silica gel (hexane) to give a yellow crystal **9** (4.28 g, 50%); mp 99−100 °C. ^{1}H NMR ($CDCl_3$, 300 MHz): δ 7.08 (d, J = 5.7 Hz, 2 H), 7.41 (d, J = 5.7 Hz, 2 H). ^{13}C NMR ($CDCl_3$, 75 MHz): δ 112.6, 127.5, 128.8, 130.8. MS (EI, $C_8H_4Br_2S_2$): calcd, 324.1; found, 324.

3,3′,5,5′-Tetrabromo-2,2′-bithiophene (10). Compound **9** (2.1 g, 6.48 mmol) and *N*-bromosuccinimide (2.54 g, 14 mmol) were dissolved in chloroform/acetic acid (13 mL, 1:1, v/v). The reaction mixture was refluxed for 5 h. The mixture solution was extracted with chloroform (250 mL × 3) and water (100 mL). The organic layer was dried over $MgSO_4$. After removal the solvent under reduced pressure, the residue was recrystallized from hexane to give a green solid **10** (2.54 g, 80%); mp 138−139 °C. ^{1}H NMR ($CDCl_3$, 300 MHz): δ 7.05 (s, 2 H). ^{13}C NMR ($CDCl_3$, 75 MHz): δ 112.1, 114.8, 129.5, 133.0. MS (EI, $C_8H_2Br_4S_2$): calcd, 481.6; found, 481.

3,3′-Dibromo-5,5′-bis(trimethylsilyl)-2,2′-bithiophene (11). To a solution of **10** (3.0 g, 6.22 mmol) in dry ether (75 mL) was added a 2.5 M solution of *n*-BuLi in hexane (5 mL, 12.4 mmol) dropwise at −78 °C. After the reaction was warm up to 0 °C and stirred for 6 h, chlorotrimethylsilane (1.36 g, 12.4 mmol) was added by syringe. After the solution was stirred at room temperature for 12 h, the reaction mixture was heated to reflux for 5 h. The mixture solution was extracted with ether (300 mL × 3) and water (150 mL). The collected organic layer was dried over $MgSO_4$. After removal the solvent under reduced pressure, the residue was purified by column chromatography on silica gel (hexane) to give the crude product which was recrystallized from ethanol to give a pale yellow solid **11** (2.15 g, 74%); mp 86−88 °C. ^{1}H NMR ($CDCl_3$, 300 MHz): δ 0.34 (s, 18 H), 7.16 (s, 2 H). ^{13}C NMR ($CDCl_3$, 75 MHz): δ −0.4, 112.9, 133.9, 137.0, 142.9. MS (EI, $C_{14}H_{20}Br_2S_2Si_2$): calcd, 468.4; found, 468.

4,4′-Dioctyl-2,6-bis(trimethylsilyl)dithieo[3,2-*b*:2′,3′-*d*]silole (12). To a solution of **11** (2.05 g, 4.37 mmol) in dry ether (55 mL) was added a 2.5 M solution of *n*-BuLi in hexane (3.7 mL, 9.2 mmol) dropwise at −78 °C. After stirring at −78 °C for 2 h, dichlorodioctylsilane (1.71 g, 5.25 mmol) was introduced by syringe to the solution which was then warmed up to room temperature. The reaction mixture was added 36.5 mL of THF and refluxed for 16 h. After cooling to room temperature, reaction solution was extracted with ether three times (250 mL × 3) and water (100 mL). The combined organic layer was dried over $MgSO_4$. After removal of the solvent under reduced pressure, the residue was purified by column chromatography on silica gel (hexane) to give a yellow oil **12** (1.77 g, 72%). ^{1}H NMR ($CDCl_3$, 300 MHz): δ 0.32 (s, 18 H), 0.80−0.90 (m, 10 H), 1.20−1.34 (m, 20 H), 1.34−1.46 (m, 4 H), 7.13 (s, 2 H). ^{13}C NMR ($CDCl_3$, 75 MHz): δ 0.1, 11.8, 14.1, 22.7, 24.2, 29.1, 29.2, 31.9, 33.2, 136.6, 141.0, 143.9, 154.5. MS (EI, $C_{30}H_{54}S_2Si_3$): calcd, 563.1; found, 563.

4,4′-Dioctyl-2,6-dibromodithieo[3,2-*b*:2′,3′-*d*]silole (D2). To a solution of **4** (1.77 g, 3.14 mmol) in chloroform/acetic acid (100 mL, 1:1, v/v) was added *N*-bromosuccinimide (1.12 g, 6.29 mmol) in one portion. The reaction was stirred for 16 h at room temperature. The mixture solution was extracted with dichloromethane (350 mL × 3) and water (100 mL). The combined organic layer was dried over $MgSO_4$. After removal the solvent under reduced pressure, the residue was purified by column chromatography on silica gel (hexane) to give a yellow oil **D2** (1.2 g, 66%). ^{1}H NMR ($CDCl_3$, 300 MHz): δ 0.80−0.95 (m, 10 H), 1.10−1.40 (m, 24 H), 6.99 (s, 2 H). ^{13}C NMR ($CDCl_3$, 75 MHz): δ 11.6, 14.1, 22.6, 24.0, 29.1, 29.2, 31.8, 33.1, 111.4, 132.1, 141.0, 148.8. MS (EI, $C_{24}H_{36}Br_2S_2Si$): calcd, 576.6; found, 576. Elemental analysis (%): Calcd for $C_{24}H_{36}Br_2S_2Si$: C, 50.0; H, 6.29. Found: C, 50.27; H, 6.47.

5,10-Diethyltetradecane-7,8-dione (15). A Grignard reagent was prepared by the following procedure. To a suspension of Mg (3.46 g, 14.2 mmol) and 3−4 drops of 1,2-dibromoethane in dry THF (85 mL) was slowly added 2-ethylhexyl bromide (25 g, 12.9 mmol) dropwise. To a suspension of LiBr (21.7 g, 250 mmol) in dry THF (93 mL) was added CuBr (17.83 g, 12.4 mmol) in dry THF (93 mL) to form a pale green solution. The mixture was then cooled to −100 °C by a pentane/liquid nitrogen bath. The Grignard reagent prepared above was slowly added to the LiBr/CuBr suspension, and the temperature of the solution was controlled below −75 °C. Oxalyl dichloride (6.57 g, 51.8 mmol) was then slowly added at a temperature below −70 °C. The mixture was stirred at −90 °C for 1 h and

then allowed to warm up to room temperature and quenched with saturated aqueous NH_4Cl (100 mL). The organic layer was separated and aqueous layer was extracted with ethyl acetate three times (300 mL × 3). The combined organic layer was dried over $MgSO_4$. After removal the solvent under reduced pressure, the residue was purified by column chromatography on silica gel (hexane) to give a pale yellow oil **15** (7.9 g, 45%).

5,8-Dibromo-2,3-bis(2-ethylhexyl)quinoxaline (A2). Compound **16**[28] (1 g, 3.8 mmol) and compound **15** (1.6 g, 5.6 mmol) were dissolved in acetic acid (50 mL) and stirred for 10 min at room temperature. After removal of acetic acid under reduced pressure, the residue was purified by column chromatography on silica gel (hexane/ethyl acetate, v/v, 50/1) to give a yellow oil **A2** (1.3 g, 68%). ^{1}H NMR ($CDCl_3$, 300 MHz): 0.96 (m, 12 H), 1.20−1.50 (m, 16 H), 2.10−2.23 (m, 2 H), 2.99 (d, J = 6.9 Hz, 4 H), 7.81 (s, 2 H). ^{13}C NMR ($CDCl_3$, 75 MHz): δ 10.9, 14.1, 23.0, 26.0, 28.9, 32.8, 38.1, 38.8, 123.4, 131.9, 139.0, 158.2. MS (EI, $C_{24}H_{36}Br_2N_2$): calcd, 512.4; found, 512. Elemental analysis (%): Calcd for $C_{24}H_{36}Br_2N_2$: C, 56.26; H, 7.08; N, 5.47. Found: C, 56.84; H, 7.42; N, 5.30.

2,3-Bis(2-ethylhexyl)-5,8-di(thiophen-2-yl)quinoxaline (19). Compound **18**[29] (1 g, 3.7 mmol) and compound **15** (1.56 g, 5.5 mmol) were dissolved in acetic acid (50 mL) and stirred for 10 min at room temperature. After removal of acetic acid under reduced pressure, the residue was purified by column chromatography on silica gel (hexane/ethyl acetate, v/v, 50/1) to give an orange oil **19** (1.8 g, 95%). ^{1}H NMR ($CDCl_3$, 300 MHz): δ 0.82−0.98 (m, 12 H), 1.20−1.52 (m, 16 H), 2.20−2.38 (m, 2 H), 3.03 (d, J = 6.9 Hz, 4 H), 7.17 (dd, J_1 = 5.1, J_2 = 3.6 Hz, 2 H), 7.48 (dd, J_1 = 5.1, J_2 = 0.9 Hz, 2 H), 7.84 (dd, J_1 = 3.6, J_2 = 0.9 Hz, 2 H), 8.06 (s, 2 H). ^{13}C NMR ($CDCl_3$, 75 MHz): δ 10.9, 14.1, 23.0, 26.0, 28.9, 32.9, 38.5, 39.3, 125.9, 126.0, 126.4, 128.4, 130.9, 137.0, 139.0, 155.6. MS (EI, $C_{32}H_{42}N_2S_2$): calcd, 518.8; found, 518.

5,8-Bis(5-bromothiophen-2-yl)-2,3-bis(2-ethylhexyl)quinoxaline (A3). To a solution of **19** (1.8 g, 3.5 mmol) in DMF (200 mL) was added *N*-bromosuccinimide (1.23 g, 6.9 mmol) at −10 °C. After stirring for 30 min, the reaction mixture was warmed up to room temperature and stirred for 1 h. The reaction solution was extracted with ether (300 mL × 3) and water (300 mL × 3). The organic solution was dried over $MgSO_4$. After removal the solvent under reduced pressure, the residue was purified by column chromatography on silica gel (hexane) to give an orange solid **A3** (2.23 g, 95%); mp 132−134 °C. ^{1}H NMR ($CDCl_3$, 300 MHz): 1.00 (m, 12 H), 1.20−1.52 (m, 16 H), 2.20−2.35 (m, 2 H), 3.03 (d, J = 6.9 Hz, 4 H), 7.10 (d, J = 3.9 Hz, 2H), 7.52 (d, J = 3.9 Hz, 2 H), 8.02 (s, 2 H). ^{13}C NMR ($CDCl_3$, 75 MHz): δ 10.9, 14.2, 23.0, 26.0, 28.9, 32.8, 38.7, 39.2, 116.8, 124.5, 125.0, 128.8, 130.2, 136.4, 139.7, 156.1. MS (EI, $C_{32}H_{40}Br_2N_2S_2$): calcd, 676.6; found, 676. Elemental analysis (%): Calcd for $C_{32}H_{40}Br_2N_2S_2$: C, 56.80; H, 5.96; N, 4.14. Found: C, 57.02; H, 6.50; N, 3.92.

2,3-Bis(2-ethylhexyl)thieno[3,4-*b*]pyrazine (22). Compound **21**[30] (1.09 g, 9.6 mmol) and compound **15** (2.8 g, 9.9 mmol) were dissolved in ethanol (400 mL) and stirred for 3 h at room temperature. After removal the solvent under reduced pressure, the residue was purified by column chromatography on silica gel (hexane/ethyl acetate, v/v, 60/1) to give a dark-green oil **22** (2.9 g, 84%). ^{1}H NMR ($CDCl_3$, 300 MHz): δ 0.81−1.0 (m, 12 H), 1.20−1.50 (m, 16 H), 1.94−2.04 (m, 2 H), 2.82 (d, J = 7.2 Hz, 4 H), 7.80 (s, 2 H). ^{13}C NMR ($CDCl_3$, 75 MHz): δ 10.8, 14.1, 23.0, 25.9, 28.8, 32.7, 38.5, 40.1, 115.7, 141.5, 156.2. MS (EI, $C_{22}H_{36}N_2S$): calcd, 360.6; found, 360.

5,7-Dibromo-2,3-bis(2-ethylhexyl)thieno[3,4-*b*]pyrazine (A4). To a solution of **22** (2.9 g, 8.0 mmol) in DMF (50 mL) was added *N*-bromosuccinimide (2.86 g, 16.0 mmol) at −10 °C. After stirring for 30 min, the solution mixture was warmed up to room temperature and stirred for 1 h. The reaction solution was extracted with ether (300 mL × 3) and water (100 mL). The combined organic layer was extracted with water (200 mL), and then the organic was dried over $MgSO_4$. After removal the solvent under reduced pressure, the residue was purified by column chromatography on silica gel (hexane) to give a dark-green oil **A4** (2.1 g, 50%). ^{1}H NMR ($CDCl_3$, 300 75 MHz): 0.96 (m, 12 H), 1.20−1.50 (m, 16 H), 1.94−2.05 (m, 2 H), 2.83 (d, J = 6.9 Hz, 4 H). ^{13}C NMR ($CDCl_3$, 75 MHz): δ 10.9, 14.1, 23.0, 26.0, 28.8, 32.7, 37.9, 39.5, 103.1, 139.1, 157.9. MS (EI, $C_{22}H_{34}Br_2N_2S$): calcd, 518.4; found, 518. Elemental analysis (%): Calcd for $C_{22}H_{34}Br_2N_2S$: C, 50.97; H, 6.61; N, 5.4. Found: C, 51.08; H, 7.03; N, 5.2.

General Procedures of Polymerization through the Stille Coupling Reaction via Microwave Reactor. To a 100 mL round-bottom flask was introduced **D1** (or **D2**) (0.37 mmol), **A1** (or **A2**−**A4**) (0.37 mmol), **D3**[31] (300 mg, 0.73 mmol), $Pd_2(dba)_3$ (26.8 mg, 0.029 mmol), tri(*o*-tolyl)phosphine (71.3 mg, 0.23 mmol), and chlorobenzene (24 mL). The mixture was then degassed by bubbling nitrogen for 10 min at room temperature. The round-bottom flask was placed into the microwave reactor and reacted for 45 min under 270 W. The solution was added into methanol dropwise. The precipitate was collected by filtration and washed by Soxhlet extraction with acetone, ethyl acetate, and THF sequentially for 1 week. The Pd-thiol gel (Silicycle Inc.) was added to above THF solution to remove the residual Pd catalyst. After filtration and removal of the solvent, the polymer was redissolved in THF again and added into methanol to reprecipitate out. The purified polymer was collected by filtration and dried under vacuum for 1 day.

P1. Dark green solid (160 mg, yield 62.3%, M_n = 26 kDa, PDI = 2.5). ^{1}H NMR ($CDCl_3$, 300 MHz): δ 0.50−0.80 (m, 12 H), 0.80−1.20 (m, 18 H), 1.80−2.10 (m, 4 H), 6.90−7.10 (m, 6 H), 7.10−7.20 (m, 2 H). FT-IR (KBr, cm^{-1}): 2951, 2914, 2852, 1626, 1558, 1501, 1477, 1457, 1396, 1256, 1181, 1079, 1063, 1011, 855, 823, 717, 692, 513.

P2. Deep red solid (160 mg, yield 47.5%, M_n = 27 kDa, PDI = 2.2). ^{1}H NMR ($CDCl_3$, 300 MHz): δ 0.40−1.70 (m, 58 H), 1.80−2.10 (m, 4 H), 2.30−2.60 (m, 2 H), 2.80−3.30 (m, 4 H), 6.90−7.10 (m, 2 H), 7.10−7.21 (m, 4 H), 8.05−8.20 (m, 2 H). FT-IR (KBr, cm^{-1}): 2957, 2924, 2871, 2855, 1628, 1458, 1260, 1071, 1036, 796.

P3. Red solid (180 mg, yield 22.7%, M_n = 19 kDa, PDI = 2.0). ^{1}H NMR ($CDCl_3$, 300 MHz): δ 0.40−1.70 (m, 58 H), 1.80−2.10 (m, 4 H), 2.30−2.60 (m, 2 H), 2.95−3.20 (m, 4 H), 6.90−7.10 (m, 2 H), 7.10−7.21 (m, 4 H), 7.50−7.80 (m, 4 H), 8.00−8.20 (m, 2 H). FT-IR (KBr, cm^{-1}): 2953, 2920, 2863, 1689, 1595, 1473, 1395, 1260, 1224, 1154, 1095, 1032, 808, 678, 616, 511.

P4. Black solid (250 mg, yield 47.2%, M_n = 36 kDa, PDI = 2.2). ^{1}H NMR ($CDCl_3$, 300 MHz): δ 0.50−1.60 (m, 60 H), 1.80−2.05 (m, 4 H), 2.70−3.05 (m, 4 H), 7.00−7.10 (m, 2 H), 7.10−7.21 (m, 4 H). FT-IR (KBr, cm^{-1}): 3061, 3026, 2953, 2924, 2868, 1454, 1376, 1259, 1172, 1071, 1032, 787, 769, 700.

P5. Dark green solid (120 mg, yield 45.7%, M_n = 22 kDa, PDI = 1.7). ^{1}H NMR ($CDCl_3$, 300 MHz): δ 0.40−1.50 (m, 34 H), 6.90−7.30 (m, 8 H). FT-IR (KBr, cm^{-1}): 3057, 2955, 2921, 2852, 1634, 1459, 1341, 1259, 1166, 1152, 1069, 833, 793.

P6. Green solid (210 mg, yield 61.3%, M_n = 44 kDa, PDI = 2.2). ^{1}H NMR ($CDCl_3$, 300 MHz): δ 0.40−1.50 (m, 62 H), 2.30−2.60 (m, 2 H), 2.80−3.30 (m, 4 H), 7.00−7.20 (m, 8 H), 8.00−8.30 (m, 2 H). FT-IR (KBr, cm^{-1}): 3056, 2958, 2919, 2850, 1749, 1637, 1481, 1441, 1344, 1260, 1167, 1019, 875, 798, 686.

Acknowledgment. This work is supported by the National Science Council and "Aim for the Top University Plan" of the National Chiao Tung University and Ministry of Education, Taiwan.

Supporting Information Available: ^{1}H and ^{13}C NMR, IR spectra, and GPC chromatograms. This material is available free of charge via the Internet at http://pubs.acs.org.

References and Notes

(1) (a) Brabec, C. J.; Sariciftci, N. S.; Hummelen, J. C. *Adv. Funct. Mater.* **2001**, *11*, 15. (b) Günes, S.; Neugebauer, H.; Sariciftci, N. S. *Chem. Rev.* **2007**, *107*, 1324.

(2) Yu, G.; Gao, J.; Hummelen, J. C.; Wudl, F.; Heeger, A. J. *Science* **1995**, *270*, 1789.

(3) Hummelen, J. C.; Knight, B. W.; LePeg, F.; Wudl, F. *J. Org. Chem.* **1995**, *60*, 532.

(4) (a) Sariciftci, N. S.; Smilowitz, L.; Heeger, A. J.; Wudl, F. *Science* **1992**, *258*, 1474. (b) Brabec, C. J.; Zerza, G.; Cerullo, G.; Silvestri, S. D.; Luzatti, S.; Hummelen, J. C.; Sariciftci, S. *Chem. Phys. Lett.* **2001**, *340*, 232. (c) Singh, T. B.; Marjanović, N.; Matt, G. J.; Günes, S.; Sariciftci, N. S.; Ramil, A. M.; Andreev, A.; Sitter, H.; Schwödiauer, R.; Bauer, S. *Org. Electron.* **2005**, *6*, 105. (d) Zhang, Y.; Yip, H.-L.; Acton, O.; Hau, S. K.; Huang, F.; Jen, A. K.-Y. *Chem. Mater.* **2009**, *21*, 2598.

(5) (a) Kitamura, C.; Tanaka, S.; Yamashita, Y. *Chem. Mater.* **1996**, *8*, 570. (b) Yamamoto, T.; Zhou, Z.-H.; Kanbara, T.; Shimura, M.; Kizu, K.; Maruyama, T.; Nakamura, Y.; Fukuda, T.; Lee, B.-L.; Ooba, N.; Tomaru, S.; Kurihara, T.; Kaino, T.; Kubota, K.; Sasaki, S. *J. Am. Chem. Soc.* **1996**, *118*, 10389.

(6) (a) Coppo, P.; Turner, M. L. *J. Mater. Chem.* **2005**, *15*, 1123. (b) Coppo, P.; Cupertino, D. C.; Yeates, S. G.; Turner, M. L. *Macromolecules* **2003**, *36*, 2705.

(7) (a) Liu, M. S.; Luo, J.; Jen, A. K.-Y. *Chem. Mater.* **2003**, *15*, 3496. (b) Luo, J.; Xie, Z.; Lam, J. W. Y.; Cheng, L.; Chen, H.; Qiu, C.; Kwok, H. S.; Zhan, X.; Liu, Y.; Zhu, D.; Tang, B. Z. *Chem. Commun.* **2001**, 1740. (c) Chen, J.; Cao, Y. *Macromol. Rapid Commun.* **2007**, *28*, 1714.

(8) (a) Zhu, Z.; Waller, D.; Gaudiana, R.; Morana, M.; Mühlbacher, D.; Scharber, M.; Brabec, C. *Macromolecules* **2007**, *40*, 1981. (b) Mühlbacher, D.; Scharber, M.; Zhengguo, M. M.; Zhu, M. M. Z.; Waller, D.; Gaudiana, R.; Brabec, C. *Adv. Mater.* **2006**, *18*, 2884. (c) Moulé, A. J.; Tsami, A.; Bünnagel, T. W.; Forster, M.; Kronenberg, N. M.; Scharber, M.; Koppe, M.; Morana, M.; Brabec, C. J.; Meerholz, K.; Scherf, U. *Chem. Mater.* **2008**, *20*, 4045. (d) Hou, J.; Chen, H. Y.; Zhang, S.; Li, G.; Yang, Y. *J. Am. Chem. Soc.* **2008**, *130*, 16144. (e) Liao, L.; Dai, L.; Smith, A.; Durstock, M.; Lu, J.; Ding, J.; Tao, Y. *Macromolecules* **2007**, *40*, 9406. (f) Hou, J.; Chen, T. L.; Zhang, S.; Chen, H.-Y.; Yang, Y. *J. Phys. Chem. C* **2009**, *113*, 1601. (g) Huo, L.; Hou, J.; Chen, H.-Y.; Zhang, S.; Jiang, Y.; Chen, T. L.; Yang, Y. *Macromolecules* **2009**, *42*, 6564.

(9) (a) Campbell, A. J.; Bradley, D. D. C.; Antoniadis, H. *Appl. Phys. Lett.* **2001**, *79*, 2133. (b) Hou, J.; Chen, T. L.; Zhang, S.; Chen, H.-Y.; Yang, Y. *J. Phys. Chem. C* **2009**, *113*, 1601.

(10) (a) Zhou, Q.; Hou, Q.; Zheng, L.; Deng, X.; Yu, G.; Cao, Y. *Appl. Phys. Lett.* **2004**, *84*, 1653. (b) Chen, C. P.; Chan, S. H.; Chao, T. C.; Ting, C.; Ko, B. T. *J. Am. Chem. Soc.* **2008**, *130*, 12828. (c) Peng, Q.; Park, K.; Lin, T.; Durstock, M.; Dai, L. *J. Phys. Chem. B* **2008**, *112*, 2801. (d) Zhao, C.; Chen, X.; Zhang, Y.; Ng, M.-K. *J. Polym. Sci., Part A: Polym. Chem.* **2008**, *46*, 2680. (e) Herguth, P.; Jiang, X.; Liu, M. S.; Jen, A. K.-Y. *Macromolecules* **2002**, *35*, 6094.

(11) Beaujuge, P. M.; Pisula, W.; Tsao, H. N.; Ellinger, S.; Küllen, K.; Reynolds, J. R. *J. Am. Chem. Soc.* **2009**, *131*, 7614.

(12) Kim, J. Y.; Lee, K.; Coates, N. E.; Moses, D.; Nguyen, T.-Q.; Dante, M.; Heeger, A. J. *Science* **2007**, *317*, 222.

(13) Kim, Y.; Shin, M.; Kim, H.; Ha, Y.; Ha, C.-S. *J. Phys. D: Appl. Phys.* **2008**, *41*, 225101.

(14) (a) Burke, K. B.; Belcher, W. J.; Thomsen, L.; Watts, B.; McNeill, C. R.; Ade, H.; Dastoor, P. C. *Macromolecules* **2009**, *42*, 3098. (b) Kim, H.; Shin, M.; Kim, Y. *J. Phys. Chem. C* **2009**, *113*, 1620. (c) Kim, Y.; Cook, S.; Choulis, S. A.; Nelson, J.; Durrant, J. R.; Bradley, D. D. C. *Synth. Met.* **2005**, *152*, 105.

(15) (a) Honda, S.; Nogami, T.; Ohkita, H.; Benten, H.; Tto, S. *Appl. Mater. Interfaces* **2009**, *1*, 804. (b) Dastoor, P. C.; McNeill, C. R.; Frohne, H.; Foster, C. J.; Dean, B.; Fell, C. J.; Belcher, W. J.; Campbell, W. M.; Officer, D. L.; Blake, I. M.; Thordarson, P.; Crossley, M. J.; Hush, N. S.; Reimers, J. R. *J. Phys. Chem. C* **2007**, *111*, 15415. (c) Johansson, E. M. J.; Yartsev, A.; Rensmo, H.; Sundström, V. *J. Phys. Chem. C* **2009**, *113*, 3014.

(16) (a) Lucas, P.; Mehdi, N. E.; Ho, H. A.; Bélanger, D.; Breau, L. *Synthesis* **2000**, *9*, 1253. (b) Beyer, R.; Kalaji, M.; Kingscote-Burton, G.; Murphy, P. J.; Pereira, V. M. S. C.; Taylor, D. M.; Williams, G. O. *Synth. Mater.* **1998**, *92*, 95. (c) Jeffries, A. T.; Moore, K. C.; Ondeyka, D. M.; Springsteen, A. W.; MacDowell, D. W. H. *J. Org. Chem.* **1981**, *46*, 2885. (d) Kraak, A.; Wiersema, A. K.; Jordens, P.; Wynberg, H. *Tetrahedron* **1968**, *24*, 3381.

(17) Brzeziński, J. Z.; Reynolds, J. R. *Synthesis* **2002**, *8*, 1053.

(18) Tierney, S.; Heeney, M.; McCulloch, I. *Synth. Met.* **2005**, *148*, 195.

(19) Brédas, J. L. *J. Chem. Phys.* **1985**, *82*, 3808.

(20) (a) Hou, J.; Park, M. H.; Zhang, S.; Yao, Y.; Chen, L. M.; Li, J. H.; Yang, Y. *Macromolecules* **2008**, *41*, 6012. (b) Tsai, J.-H.; Chueh, C.-C.; Lai, M.-H.; Wang, C.-F.; Chen, W.-C.; Ko, B.-T.; Ting, C. *Macromolecules* **2009**, *42*, 1897. (c) Lee, W.-Y.; Cheng, K.-F.; Wang, T.-F.; Chueh, C.-C.; Chen, W.-C.; Tuan, C.-S.; Lin, J.-L. *Macromol. Chem. Phys.* **2007**, *208*, 1919.

(21) Ono, K.; Tanaka, S.; Yamashita, Y. *Angew. Chem., Int. Ed.* **1994**, *33*, 1977.

(22) Karikomi, M.; Kitamura, C.; Tanaka, S.; Yamashita, Y. *J. Am. Chem. Soc.* **1995**, *117*, 6791.

(23) (a) Wienk, M. M.; Kroon, J. M.; Verhees, W. J. H.; Knol, J.; Hummelen, J. C.; van Hal, P. A.; Janssen, R. A. J. *Angew. Chem., Int. Ed.* **2003**, *42*, 3371. (b) Yao, Y.; Shi, C.; Li, G.; Shrotriya, V.; Pei, Z.; Yang, Y. *Appl. Phys. Lett.* **2006**, *89*, 153507.

(24) (a) Brabec, C. J.; Cravino, A.; Meissner, D.; Sariciftci, N. S.; Rispens, M. T.; Sanchez, L.; Hummelen, J. C.; Fromherz, T. *Thin Solid Films* **2002**, *403*, 368. (b) Mihailetchi, V. D.; P. Blom, W. M.; Hummelen, J. C.; Rispens, M. T. *J. Appl. Phys.* **2003**, *94*, 6849.

(25) Mühlbacher, D.; Scharber, M.; Morana, M.; Zhu, Z.; Waller, D.; Gaudiana, R.; Brabec, C. *Adv. Mater.* **2006**, *18*, 2884.

(26) Erb, T.; Zhokhavets, U.; Gobsch, G.; Raleva, S.; Stuhn, B.; Schilinsky, P.; Waldauf, C.; Brabec, C. J. *Adv. Funct. Mater.* **2005**, *15*, 1193.

(27) Chen, H.-Y.; Hou, J.; Hayden, A. E.; Yang, H.; Houk, K. N.; Yang, Y. *Adv. Mater.* **2009**, in press.

(28) Yang, R.; Tian, R.; Yan, J.; Zhang, Y.; Yang, J.; Hou, Q.; Yang, W.; Zhang, C.; Cao, Y. *Macromolecules* **2005**, *38*, 244.

(29) Kitamura, C.; Tanaka, S.; Yamashita, Y. *Chem. Mater.* **1996**, *8*, 570.

(30) Kenning, D. D.; Mitchell, K. A.; Calhoun, T. R.; Funfar, M. R.; Sattler, D. J.; Rasmussen, S. C. *J. Org. Chem.* **2002**, *67*, 9073.

(31) Van, P. C.; Macomber, R. S.; Mark, H. B., Jr.; Zimmer, H. *J. Org. Chem.* **1984**, *49*, 5250.